Penerbit Akademia Baru

Journal of Advanced Research in Fluid Mechanics and Thermal Sciences

Journal homepage: www.akademiabaru.com/arfmts.html
ISSN: 2289-7879

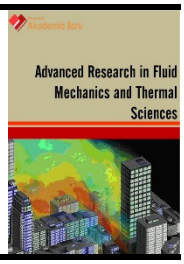

The investigation on SIMPLE and SIMPLER algorithm through lid driven cavity

Open

Lee Chern Earn [1], Tey Wah Yen[*,1,2] , Tan Lit Ken [2]

[1] Department of Mechanical Engineering, Faculty of Engineering, UCSI University Kuala Lumpur, Malaysia
[2] Malaysia-Japan International Institute of Technology (MJIIT), Universiti Teknologi Malaysia Kuala Lumpur, Malaysia

ARTICLE INFO

Article history:
Received 9 January 2017
Received in revised form 6 February 2017
Accepted 7 February 2017
Available online 16 February 2017

Keywords:
SIMPLE algorithm, SIMPLER algorithm, Lid driven cavity, Navier-Stokes equations, Computational cost

ABSTRACT

The present study analyzes in details to compare SIMPLE and SIMPLER algorithm in terms of their convergence rate, iteration number and computational time. The work which is based on primitive variables (u, v, P) formulation of Navier-Stokes equations to investigate the velocity and pressure distribution in the square cavity at Reynolds number of 100 and 400. The solutions are obtained for grid size 16 × 16 up to 256 × 256. From the plots of velocity profiles along centerline geometry, it shows good agreement with the benchmark solution from past researchers. The velocity and pressure in the cavity varies as the Reynolds number increases from 100 to 400. SIMPLER algorithm is proven to be more efficient compared to SIMPLE as iteration number required for a given Reynolds number and grid size is lower than that of SIMPLE. The values of under-relaxation factors for velocity components and pressure play significant role in terms of convergence rate of a numerical scheme.

1. Introduction

Lid driven cavity [1,2] is a classic benchmark problem for viscous incompressible flow [3-5]. The model is able to exhibit various types of phenomena that can happen in an incompressible flow such as secondary flows, transition to turbulence, eddy flows and complex three-dimensional patterns [6,7]. In order to solve the incompressible Navier-Stokes equations, various methods have been developed and the commonly used numerical procedure is Semi-Implicit Method for Pressure Linked Equation (SIMPLE) and SIMPLER (SIMPLE – Revised) by [8].

Yapici and Uludag [9] have used finite volume method (FVM) of two-dimensional square lid driven cavity flow at high Reynolds number (*Re*). The coupled flow equation is solved by SIMPLE algorithm. Moreover, he has used QUICK scheme to approximate the convection terms in the flow equations.

[*] *Corresponding author.*
E-mail address: teywy@ucsiuniversity.edu.my (W.Y. Tey)

In the findings, the accuracy of a numerical solution can be improved by using a smaller mesh in the regions of high gradients than the mesh size of bulk flow.

Jing Yang *et al.* [10] have presented a model for pool boiling called CAS model. The numerical model is commonly used to measure the heat transfer in the industries application. SIMPLER algorithm is integrated with a cellular automata technique to investigate the pressure and temperature during the boiling process as the cellular automata technique alone is not effective to investigate the boiling process. From the results shown, the integration of the technique into the algorithm has proven to be a good approach in obtaining data coherent with the benchmark solution.

Yin and Chow [11] have computed comparison of four algorithms in simulating atrium fire. The four algorithms for solving the velocity-pressure coupled equations are SIMPLE, SIMPLER, SIMPLEC and PISO. The numerical schemes are each tested with the relaxation factors. In the results, all four algorithms provide similar data for the flow variables except for pressure. It is concluded in the studies that SIMPLER is the viable algorithms used to solve the equations in simulating atrium fire.

Although SIMPLE and SIMPLER method is widely used to solve velocity-pressure coupling fluid problems, the numerical comparison between them is still unclear. Hence, the objective of the present study is to compare SIMPLE and SIMPLER in terms of convergence, iteration number and computational time.

2. Numerical details

2.1. The governing equations

The incompressible two-dimensional Navier-Stokes equations can be written as follows:

$$\rho\left(\frac{\partial u}{\partial t}+\frac{\partial uu}{\partial x}+\frac{\partial uv}{\partial y}\right)=-\frac{\partial P}{\partial x}+\mu\nabla^2 u \tag{1}$$

$$\rho\left(\frac{\partial v}{\partial t}+\frac{\partial vv}{\partial y}+\frac{\partial uv}{\partial x}\right)=-\frac{\partial P}{\partial y}+\mu\nabla^2 v \tag{2}$$

$$\frac{\partial u}{\partial x}+\frac{\partial v}{\partial y}=0 \tag{3}$$

with $\nabla= i\frac{\partial}{\partial x}+j\frac{\partial}{\partial y}$. Expanding the terms on x- and y-momentum equations results in:

$$\rho\left(\frac{\partial u}{\partial t}+\frac{\partial uu}{\partial x}+\frac{\partial uv}{\partial y}\right)=-\frac{\partial P}{\partial x}+\mu\left(\frac{\partial^2 u}{\partial x^2}+\frac{\partial^2 u}{\partial y^2}\right) \tag{4}$$

$$\rho\left(\frac{\partial v}{\partial t}+\frac{\partial vv}{\partial y}+\frac{\partial uv}{\partial x}\right)=-\frac{\partial P}{\partial y}+\mu\left(\frac{\partial^2 v}{\partial x^2}+\frac{\partial^2 v}{\partial y^2}\right) \tag{5}$$

Based on Eq.s (3) – (5), a general transport equation can be written as follows:

$$\frac{\partial}{\partial t}(\rho\emptyset)+\frac{\partial}{\partial x}(\rho u\emptyset)+\frac{\partial}{\partial y}(\rho v\emptyset)=\frac{\partial}{\partial x}\left(\Gamma\frac{\partial\emptyset}{\partial x}\right)+\frac{\partial}{\partial y}\left(\Gamma\frac{\partial\emptyset}{\partial y}\right)+S_\emptyset \tag{6}$$

where$\emptyset$ is the dependent variable such as velocity, temperature and enthalpy, Γ is the diffusion coefficient and $S_\emptyset$ represent the source term. The first term on LHS is the unsteady term and the second and third term on LHS is the convection terms. Consider only the x-momentum equation, the

Ø in Eq. 6 is replaced by u-velocity. Using discretization method by staggered grid as explained in detail by [4,10], discretized *x*-momentum equation is as follows:

$$a_P u_P = a_E u_E + a_W u_W + a_N u_N + a_S u_S + b_u = \sum_{nb} a_{nb} u_{nb} + b_u \quad (7)$$

where the coefficient a_E, a_W, a_N, a_S are the convection – diffusion at the neighboring cell faces and $b_u = (p_e - p_w) + S_e \Delta x \Delta y$.

2.2. SIMPLE algorithm

The Semi-Implicit Method for Pressure-Linked Equations (SIMPLE) is originally proposed by [8]. The principle of SIMPLE is to create discrete pressure equation based on discrete continuity equation. The *u*-momentum equation for control volume centred at e is given as:

$$a_e u_e = \sum_{nb} a_{nb} u_{nb} + A_e (P - P_E) + b_e \quad (8)$$

A guessed pressure field denoted as *P** is to replace onto the Eq. 8 to obtain guessed velocity components of *u** and *v**:

$$a_e u_e^* = \sum_{nb} a_{nb} u_{nb}^* + A_e (P_P^* - P_E^*) + b_e \quad (9)$$

However, the guessed velocity components would not able to satisfy conservation of mass, in that case, velocity and pressure are corrected by adding correction values:

$$\begin{aligned} u &= u^* + u' \\ P &= P^* + P' \\ v &= v^* + v' \end{aligned} \quad (10)$$

Relating Eq.s 8 - 10 gives:

$$a_e u_e' = \sum_{nb} a_{nb} u_{nb}' + A_e (P_P' - P_E') \quad (11)$$

The neighbouring values in Eq. 11 are omitted for approximation as the terms will not affect the final solution due to the correction values, *u'* will be zero when the solution converged. Then, relating to Eq. 10 becomes:

$$u_e = u_e^* + d_e (P_P' - P_E') \quad (12)$$

At this point, Eq. 12 is needed to satisfy the discretized continuity equation $(\rho u A)_e - (\rho u A)_w + (\rho v A)_n - (\rho v A)_s = 0$, hence it is substitute into the continuity equation. The same goes for u_w, u_n, u_s which gives:

$$[(\rho dA)_e + (\rho dA)_w + (\rho dA)_n + (\rho dA)_n] P_P' = (\rho dA)_e P_E' + (\rho dA)_w P_W' + (\rho dA)_n P_N' + (\rho dA)_s P_S' + [(\rho u^* A)_w - (\rho u^* A)_e + (\rho u^* A)_s - (\rho u^* A)_n] = 0 \quad (13)$$

Simplifying Eq. 13 leads to:

$$a_P P'_P = a_E P'_E + a_W P'_W + a_N P'_N + a_S P'_S + b'_P \quad (14)$$

where,

$a_E = (\rho dA)_e$

$a_w = (\rho dA)_w$

$$a_N = (\rho dA)_n$$
$$a_S = (\rho dA)_s$$
$$a_P = \sum_{nb} a_{nb}$$
$$b'_P = (\rho u^* A)_w - (\rho u^* A)_e + (\rho u^* A)_s - (\rho u^* A)_n$$

Eq. 14 is a pressure correction equation, the momentum source term *b'* is the mass imbalance due to incorrect velocity field. When the source term reaches zero, it means that the solution has converge.

2.3. SIMPLER algorithm

SIMPLER is a revised version of SIMPLE in which discretized continuity equation is used to derived discretized equation for pressure instead of pressure correction equation. Pseudo-velocities are introduced in SIMPLER, which can be defined as follows:

$$\hat{u}_e = \frac{\sum_{nb} a_{nb} u_{nb} + b_e}{a_e} \quad (15)$$

Substitute Eq. 15 into Eq. 8 gives:

$$u_e = \hat{u}_e + d_e(p_P - p_E) \quad (16)$$

Substitute Eq. 16 into discretized continuity equation and rearranging the terms produces:

$$[(\rho dA)_e + (\rho dA)_w + (\rho dA)_n + (\rho dA)_n]p'_P = (\rho dA)_e p_E + (\rho dA)_w p_W + (\rho dA)_n p_N + (\rho dA)_s p_S + [(\rho \hat{u} A)_w - (\rho \hat{u} A)_e + (\rho \hat{v} A)_s - (\rho \hat{v} A)_n] \quad (17)$$

Eq. 17 can be further simplified into:

$$a_P p_P = a_E p_E + a_W p_W + a_N p_N + a_S p_S + b_P \quad (18)$$

where

$a_E = (\rho dA)_e$

$a_w = (\rho dA)_w$

$a_N = (\rho dA)_n$

$a_S = (\rho dA)_s$

$a_P = \sum_{nb} a_{nb}$

$b'_P = (\rho \hat{u} A)_w - (\rho \hat{u} A)_e + (\rho \hat{v} A)_s - (\rho \hat{v} A)_n$

After obtaining the pressure value, the following sequence is the same as SIMPLE in which the pressure value is used to solve the discretized momentum equation.

3. Results and discussion

3.1. Mesh independence study and validation

Prior to comparative study on computational efficiency of SIMPLE and SIMPLER model, the validation is done by comparing the computed velocity value with the work of [13].

Extrema of velocity along geometry centreline at *Re* = 100 and *Re* = 400 are tabulated in Table 1 and Table 2. It is shown that both algorithms are able to produce results that are good agreement with Ghia's benchmark solution [13] as the grid increases. It can be said that grid independence is achieved in this case.

For SIMPLE algorithm, the Navier-Stokes equations can only be solved up to 128 × 128 grid due to the under-relaxation factors. Optimal value of relaxation factors could not be obtained, hence, the solution oscillates and diverge at one point of the iteration. In the present study, convergence criterion is set as 10^{-3} at which the simulation is terminated and assumed to reach steady state. The convergence criterion defined in the present study is the summation of error of velocity components and pressure,

$$\epsilon = \sum \left| \emptyset^{n+1} - \emptyset^{n} \right| \leq 10^{-3} \tag{19}$$

where Ø represents primitive variables, n is the iteration step.

Table 1
Extrema of velocity along geometry centerline at Re = 100

Reference	Grid	u_{min}	v_{max}	v_{min}
SIMPLE	16 × 16	-0.18011	0.14960	-0.20606
SIMPLER	16 × 16	-0.18741	0.16002	-0.23098
SIMPLE	32 × 32	-0.20687	0.17349	-0.24592
SIMPLER	32 × 32	-0.20555	0.17387	-0.24588
SIMPLE	64 × 64	-0.21265	0.17834	-0.25247
SIMPLER	64 × 64	-0.21183	0.17810	-0.25167
SIMPLE	128 × 128	-0.21373	0.17932	-0.25356
SIMPLER	128 × 128	-0.21349	0.17924	-0.25335
SIMPLER	256 × 256	-0.21391	0.17950	-0.25371
Ghia et. al. [13]	129 × 129	-0.21090	0.17527	-0.24533

Table 2
Extrema of velocity along geometry centerline at Re = 400

Reference	Grid	u_{min}	v_{max}	v_{min}
SIMPLE	16 × 16	-0.17234	0.16559	-0.28274
SIMPLER	16 ×16	-0.17200	0.16585	-0.28220
SIMPLE	32 × 32	-0.24566	0.23069	-0.36796
SIMPLER	32 × 32	-0.24533	0.23085	-0.36778
SIMPLE	64 × 64	-0.29837	0.27849	-0.42560
SIMPLER	64 × 64	-0.29770	0.27749	-0.42458
SIMPLE	128 × 128	-0.31973	0.29701	-0.44629
SIMPLER	128 × 128	-0.31928	0.29602	-0.44564
SIMPLER	256 × 256	-0.32613	0.30172	-0.45178
Ghia et. al. [13]	129 × 129	-0.32726	0.30203	-0.44993

3.2. Pressure-Velocity contour plot

As both algorithms produced similar results, finest grid size of contour plots are illustratedfrom Fig. 1(a) - 1(f). With the increasing of Reynolds number from 100 to 400, the pressure in the cavity has decreases. The maximum pressure of the flow is present at the top right corner of the cavity, whereas, the minimum pressure occurs at the top left corner of the cavity. As the fluid moves from left to right on the top lid, the fluid starts to spreads throughout the cavity after knocking the right wall. The pressure is then decreases at the lower part of the cavity.

In the *u*-velocity contour plot, the velocity flow is dominant at the top lid due to stationary walls on both sides. In addition to that, it can be seen that the boundary layer of the flow near the top moving lid is thinner as the Reynolds number increases. The region of the minimum velocity has increases and shifted towards the center of the cavity.

Due to the increase of Reynolds number, the velocity components have a higher magnitude throughout the region inside the cavity. The bottom left and right corner of low velocity has covers larger region as compared to at *Re* = 100. In v-velocity contour, the fluid flow is dominant on the left wall and the flow is reverse on the right wall. At higher *Re*, the maximum and minimum *v*-velocity regions spreads out, covers larger area in the cavity.

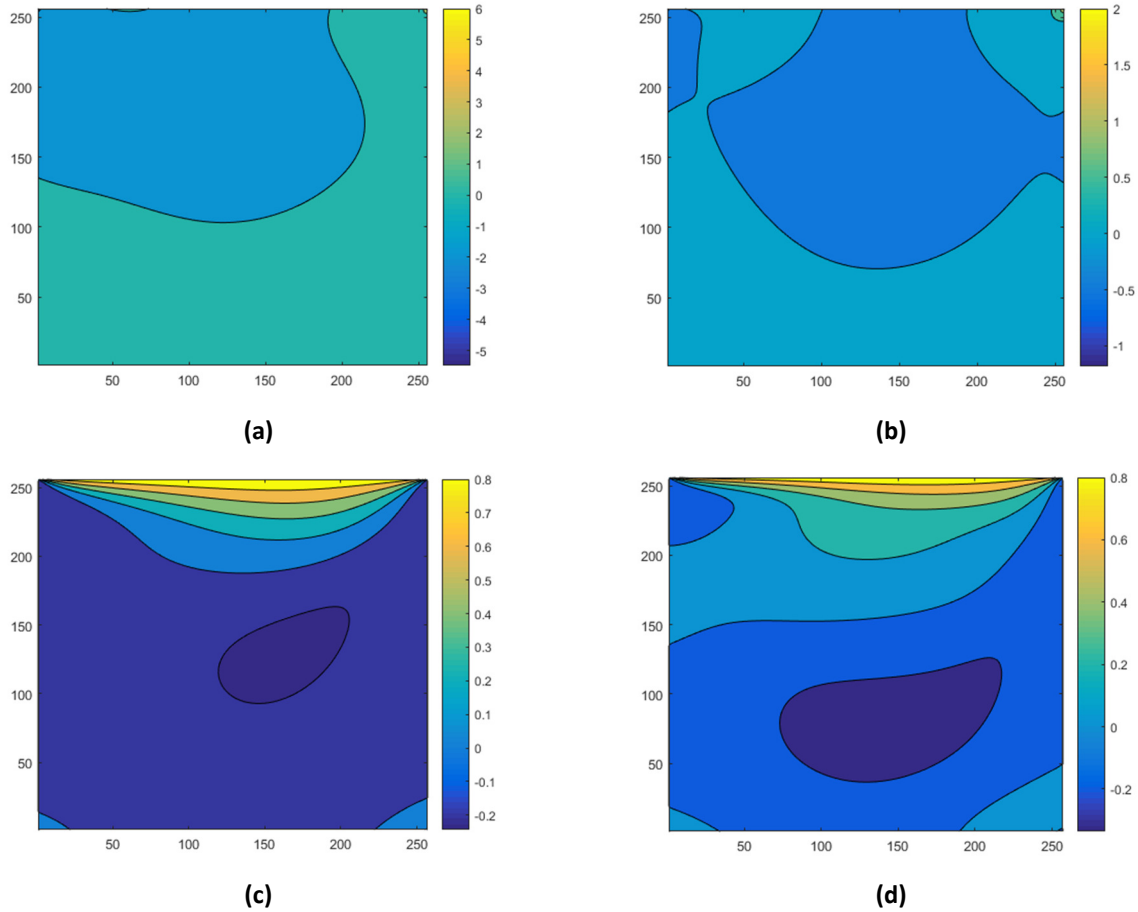

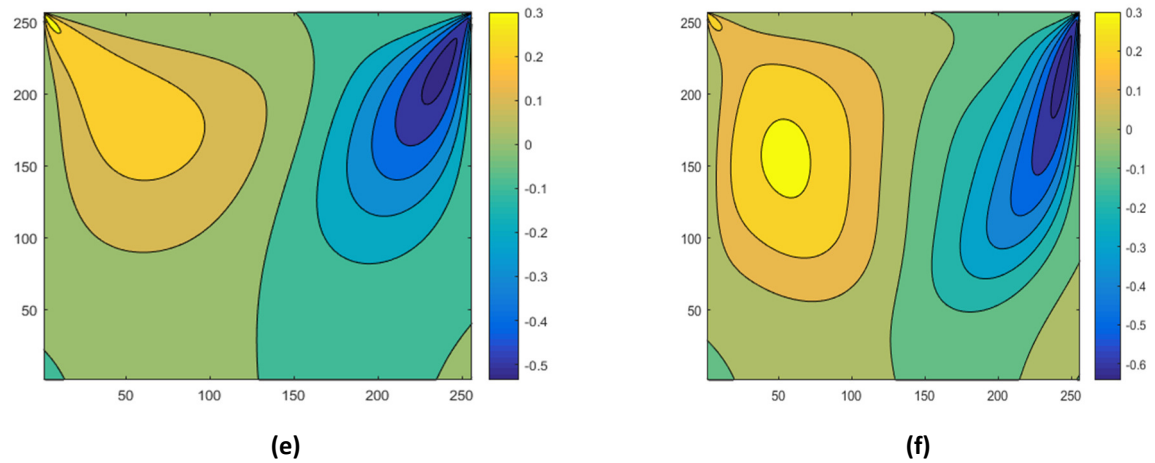

(e) **(f)**

Fig. 1. Contour plots with at 256 × 256 grid for (a) pressure, *Re* = 100; (b) pressure, *Re* = 400; (c) *u*-velocity, *Re* = 100; (d) *u*-velocity, *Re* = 400; (e) *v*-velocity, *Re* = 100; (f) *v*-velocity, *Re* = 400

3.3. Velocity profile analysis

From Fig. 2 - 5, it is shown that the *u*-velocity and *v*-velocity profile along vertical and horizontal centerline of geometry of cavity respectively are coherent with Ghia's benchmark solution as the grid size increases. However, SIMPLE algorithm unable to be implemented for 256 × 256 grid size due to incompatible relaxation factors. Optimum relaxation factors for velocity and pressure cannot be found, hence, cause the solution to oscillates and diverge.

The minimum *u*-velocity along the vertical centerline of the cavity and *v*-velocity at minimum and maximum along horizontal centerline for various grid sizes are computed in Table 3. The minimum u-velocity is denoted as u_{min} and minimum and maximum *v*-velocity are denoted as v_{min} and v_{max} respectively. As can be seen from the table, the extrema of velocity of grid size 128 × 128 and 256 × 256 of SIMPLER algorithm does not differ much. This in turns shows that, the numerical solution will no longer changes with the increasing of grid size, in other words, grid independence. Furthermore, both SIMPLE and SIMPLER algorithms have implemented and converge to similar results.

Table 3
Extrema of velocity along the centerline of the cavity, Re = 100

Reference	Grid	u_{min}	v_{max}	v_{min}
SIMPLE	16 × 16	-0.18011	0.14960	-0.20606
SIMPLER	16 ×16	-0.18741	0.16002	-0.23098
SIMPLE	32 × 32	-0.20687	0.17349	-0.24592
SIMPLER	32 × 32	-0.20555	0.17387	-0.24588
SIMPLE	64 × 64	-0.21265	0.17834	-0.25247
SIMPLER	64 × 64	-0.21183	0.17810	-0.25167
SIMPLE	128 × 128	-0.21373	0.17932	-0.25356
SIMPLER	128 × 128	-0.21349	0.17924	-0.25335
SIMPLER	256 × 256	-0.21391	0.17950	-0.25371
Ghia *et. al* [10]	129 × 129	-0.21090	0.17527	-0.24533

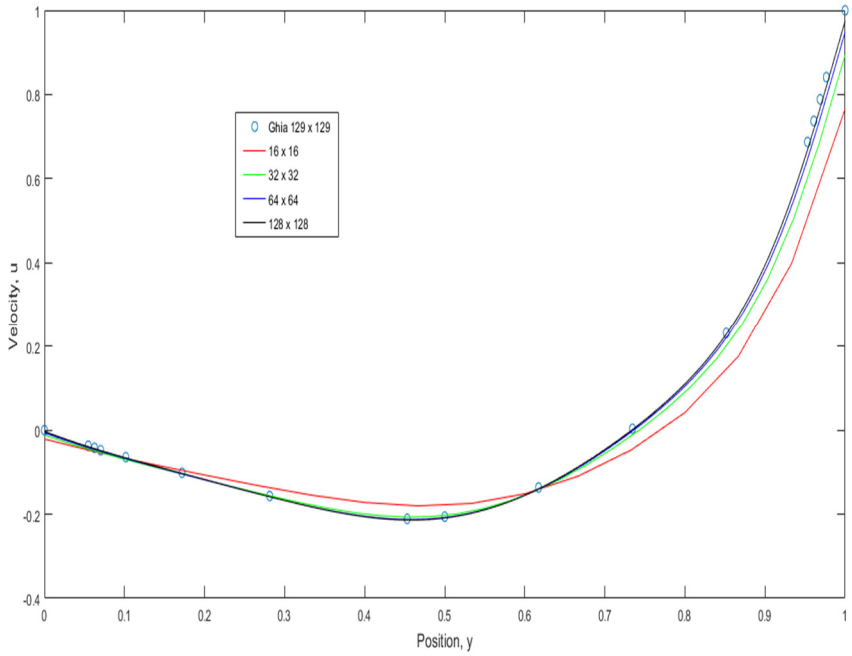

Fig. 2.U-velocity profile along vertical centerline by SIMPLE algorithm at *Re* = 100

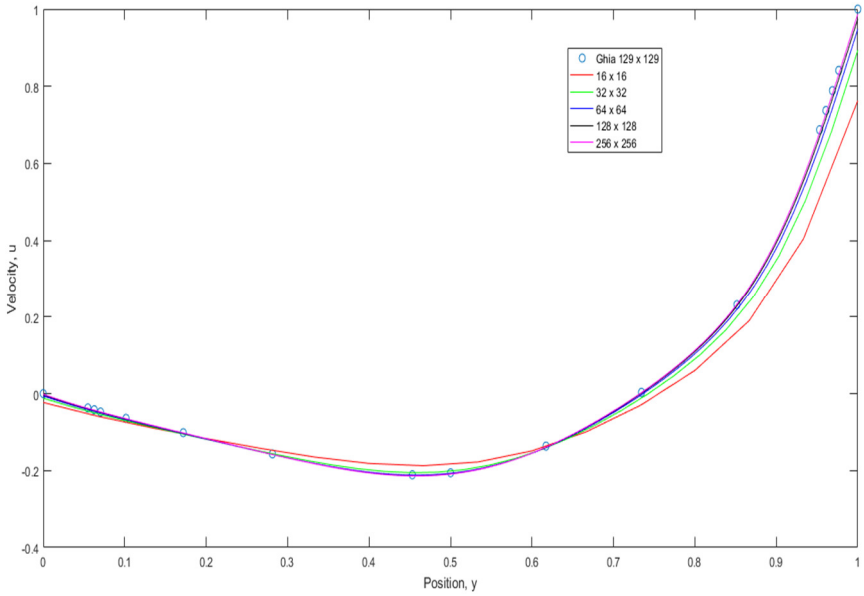

Fig. 3.V-velocity profile along vertical centerline by SIMPLE algorithm at *Re* = 100

In the simulation runs at *Re* = 400, the results obtained are also coherent with the benchmark solution as shown in Fig.s 6 - 9. Both algorithms are implemented and matches well with Ghia as the size of the grid increases. SIMPLE algorithm can only be implemented to solve up until 128 × 128 due to incompatible relaxation parameters found.

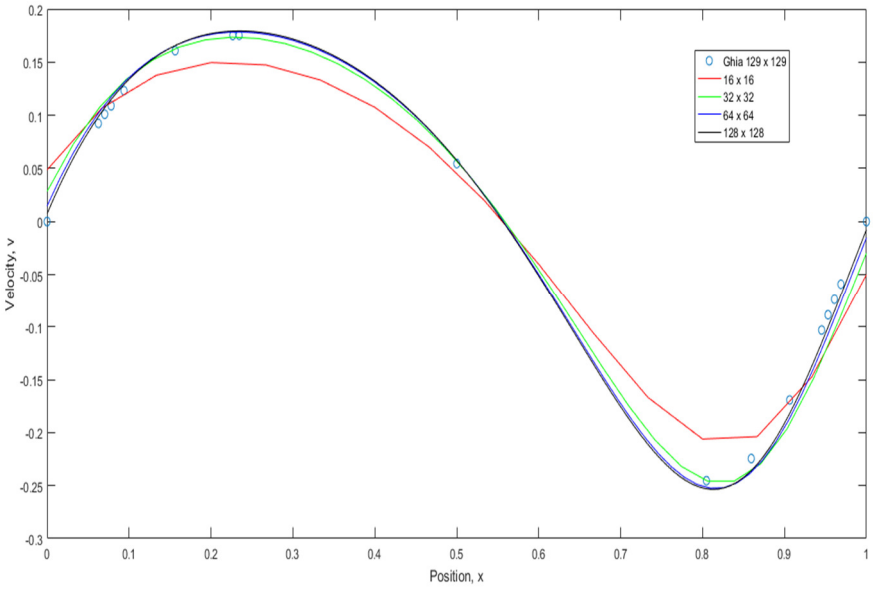

Fig. 4.U-velocity profile along horizontal centerline by SIMPLE algorithm at *Re* = 100

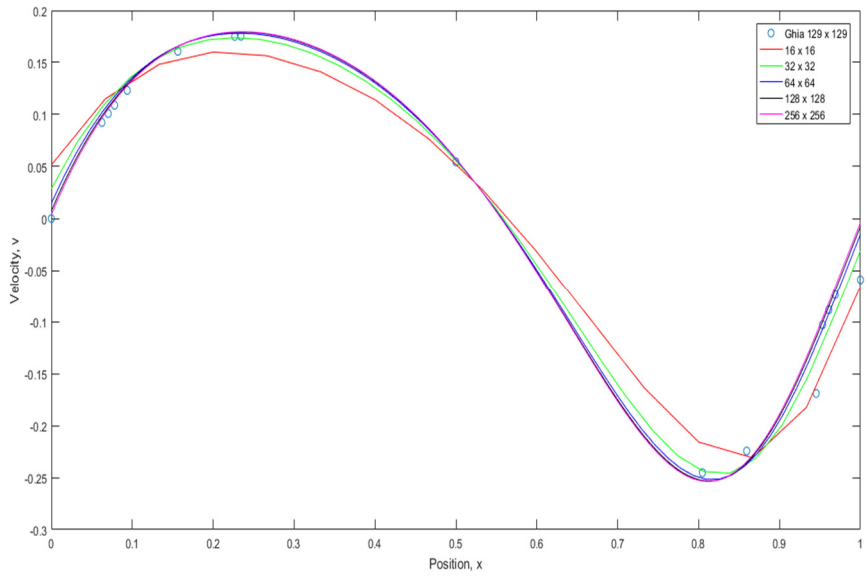

Fig. 5.V-velocity profile along horizontal centerline by SIMPLE algorithm at *Re* = 100

As previously mentioned in the results at *Re* = 100, there is not much difference in extrema velocity of grid size 128 × 128 and 256 × 256. However, at *Re* = 400, the velocity between the two grid sizes has larger difference values as compared to the solution at *Re* = 100. It can be said that for larger Reynolds number, finer grid size is required in order to reach grid independence. Similarly, both SIMPLE and SIMPLER algorithm implemented is able to converge to the same extrema velocity profiles at all grid sizes. This can be shown through Table 4.

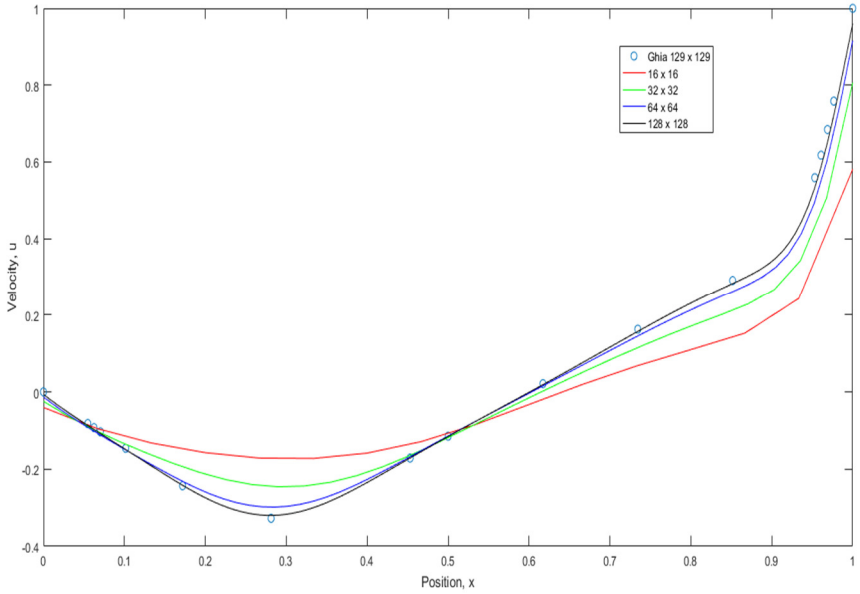

Fig. 6.U-velocity profile along vertical centerline by SIMPLE algorithm at *Re* = 400

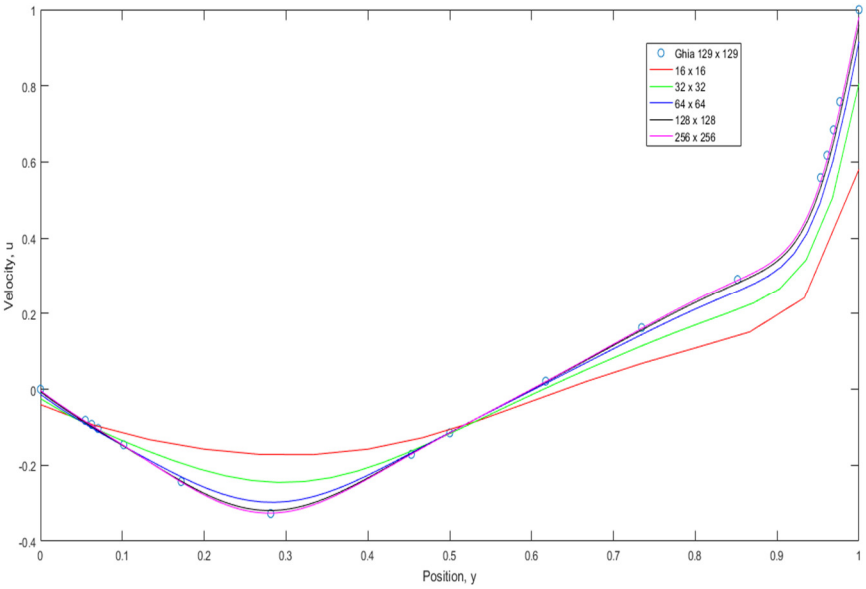

Fig. 7.V-velocity profile along vertical centerline by SIMPLE algorithm at *Re* = 400

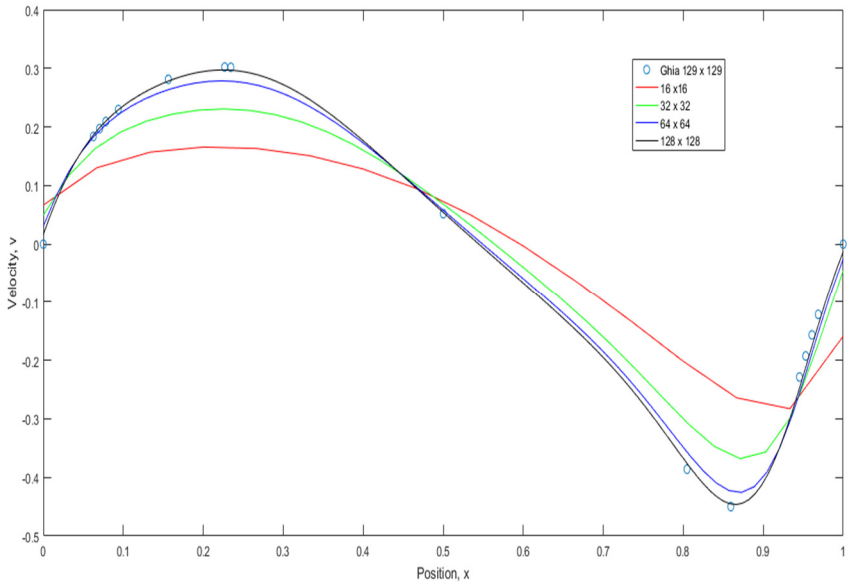

Fig. 8. U-velocity profile along horizontal centerline by SIMPLE algorithm at *Re* = 400

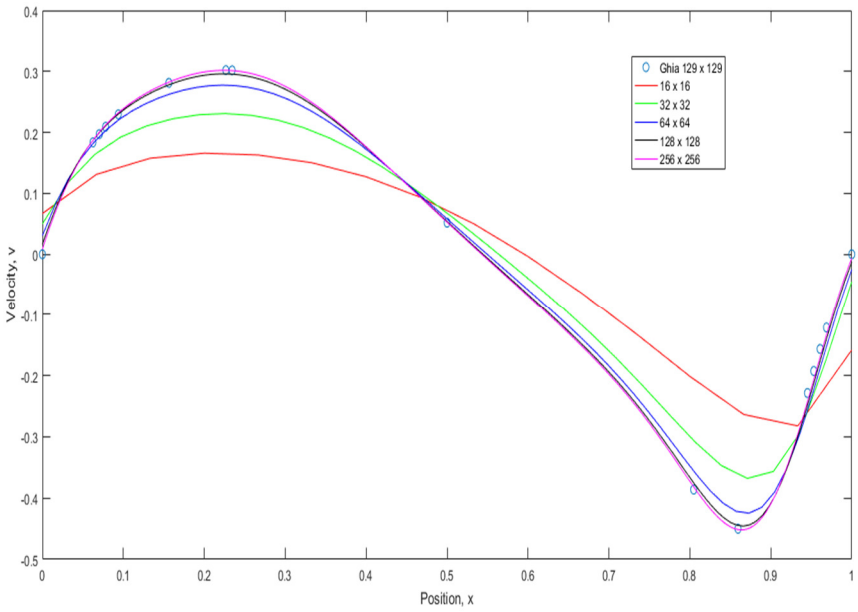

Fig. 9.V-velocity profile along horizontal centerline by SIMPLE algorithm at *Re* = 400

Table 4
Extrema of velocity along the centerline of the cavity, *Re* = 400

Reference	Grid	u_{min}	v_{max}	v_{min}
SIMPLE	16 x 16	-0.17234	0.16559	-0.28274
SIMPLER	16 x16	-0.17200	0.16585	-0.28220
SIMPLE	32 x 32	-0.24566	0.23069	-0.36796
SIMPLER	32 x 32	-0.24533	0.23085	-0.36778
SIMPLE	64 x 64	-0.29837	0.27849	-0.42560
SIMPLER	64 x 64	-0.29770	0.27749	-0.42458
SIMPLE	128 x 128	-0.31973	0.29701	-0.44629
SIMPLER	128 x 128	-0.31928	0.29602	-0.44564
SIMPLER	256 x 256	-0.32613	0.30172	-0.45178
Ghia et. al	129 x 129	-0.32726	0.30203	-0.44993

3.4. Computational Cost Study

The numerical solution is obtained on PC with Intel® Core™i5 processor and 8GB RAM. In general, it can be seen that the iteration number and computational time to implement SIMPLE is much larger than SIMPLER. For *Re* = 400 and at grid size 128 × 128, the iteration number and computational time has reach as high as 127999 and 16228.38 seconds. Whereas, for SIMPLER algorithm, it can go as fast as 1.03 seconds and only require 309 iterations to obtain the solution.

However, there is a set of values which does not follow the trend, at which at *Re* = 100 of grid size 128 × 128, the iteration number and computational time required for SIMPLER is larger than that of SIMPLE. The reason of this discrepancy is due to the relaxation factor used in the SIMPLE algorithm. As mentioned in Chapter III, the algorithm is largely dependent on the relaxation factors. For this case, the relaxation factor selected could be the optimum value for the algorithm to run at that given Reynolds number and grid size. The iteration number and computational time for SIMPLE algorithm can be improved if an optimum relaxation factor can be found.

The convergence rate between SIMPLE and SIMPLER algorithms are compared and computed in the Table 5 - 7. Referring to [14], the rate of convergence canbecalculated with the formula given as follows:

$$convergence\ rate = \log_2 \frac{\left|u_{min}^{32\times32} - u_{min}^{128\times128}\right|}{\left|u_{min}^{64\times64} - u_{min}^{128\times128}\right|} \tag{19}$$

Grid size 128 × 128 is chosen as the reference solution. The ratio of the two errors can get an estimate of the convergence. u_{min} and $v_{min}$of grid size 32 × 32, 64 × 64 and 128 × 128 at *Re* = 100 and *Re* = 400 are select from Table 1 – 2. $Rate_u$ and $Rate_v$are the convergence rate for the u_{min} and v_{min} respectively. In the table, it shows that SIMPLER algorithm implemented at *Re* = 100 and *Re* = 400 has better convergence rate as compared to SIMPLE algorithm due to the smaller ratio in error.

Table 5
Iteration number and computational time at *Re* = 100

Re = 100	Grid	Iteration Number	Computational Time (s)
SIMPLE	16 × 16	7039	17.17
SIMPLER	16 × 16	309	1.03
SIMPLE	32 × 32	11974	85.87
SIMPLER	32 × 32	1175	12.26
SIMPLE	64 × 64	13922	305.51
SIMPLER	64 × 64	4576	146.94
SIMPLE	128 × 128	17296	1244.98
SIMPLER	128 × 128	18169	2038.38

Table 6
Iteration number and computational time at *Re* = 400

Re = 400	Grid	Iteration Number	Computational Time (s)
SIMPLE	16 × 16	2745	9.40
SIMPLER	16 × 16	437	1.12
SIMPLE	32 × 32	8366	94.54
SIMPLER	32 × 32	1321	11.94
SIMPLE	64 × 64	21069	753.22
SIMPLER	64 × 64	3840	129.86
SIMPLE	128 × 128	127999	16228.38
SIMPLER	128 × 128	13705	1542.31

Table 7
Convergence rate at *Re* = 100 and *Re* = 400

Reference	Reynolds Number	$Rate_u$	$Rate_v$
SIMPLE	100	2.667	2.809
SIMPLER	100	2.258	2.153
SIMPLE	400	1.794	1.921
SIMPLER	400	1.777	1.886

4.Conclusion

In the present work, SIMPLE and SIMPLER are employed to investigate the pressure and velocity distribution in lid driven cavity. Comparison have made between the two algorithms in terms of convergence, iteration number and computational time. Numerical solution for the incompressible flow at *Re* = 100 and *Re* = 400 up to 256 × 256 grid are computed. The results obtained compared well with the benchmark solution from previous literature. The pressure and velocity distribution changes according to the Reynolds number. The magnitude of the pressure and the location of the minimum *u*-velocity region are affected by the variation of Reynolds number. From this study, it is found that SIMPLER require less iteration number and computational time to converge solution despite the extra computational load. The findings from this study are able to be used as a reference by future researchers in the comparison of these numerical schemes.

Future improvement can be made on this study to improve the computational time of the numerical schemes. FORTRAN can be used as it is better as compared to MATLAB with its recognizable computational efficiency. This in turns improve the performance and encourages more findings at higher Reynolds number and finer grid size in shorter amount of time. In addition, an application of improvised under-relaxation method on SIMPLE algorithm can improve the convergence rate and computational time. In this way, more results can be obtained if optimal relaxation factors are used in the numerical scheme. The solution will no longer oscillates heavily or diverge.

Acknowledgement
The work is supported by Centre of Excellence for Research, Value Innovation and Entrepreneurship (CERVIE) UCSI University under University Pioneer Scientist Incentive Fund (PSIF) with project code Proj-In-FETBE-038.

References
[1] Sidik, N.A.C. and Razali, S.A. "Various speed ratios of two-sided lid-driven cavity flow using Lattice Boltzmann Method." *Journal of Advanced Research in Fluid Mechanics and Thermal Sciences* 1, no. 1 (2014): 11-18.
[2] Jahanshaloo, L., Sidik, N.A.C. and Salimi, S. "Numerical simulation of high Reynolds number flow in lid-driven cavity using multi-relaxation time Lattice Boltzmann Method." *Journal of Advanced Research in Fluid Mechanics and Thermal Sciences* 24, no. 1 (2016): 12-21.
[3] Zoran, Z., Matjaz, H., Leopol, S. and Jure, R. "3D Lid driven Cavity flow by Mixed Boundary and Finite Element Method."In: *European Conference on Computational Fluid Dynamics ECCOMAS CFD*, 2006.
[4] Kefayati, G.H.R. and Sidik, N.A.C. "Simulation of natural convection and entropy generation of non-Newtonian nanofluid in an inclined cavity using Buongiorno's mathematical model (Part II, entropy generation)." *Powder Technology* 305 (2017): 679-703.
[5] Kwon, Y.W. and Arceneaux, S.M. "Experimental study of channel driven cavity flow for fluid–structure interaction." *Journal of Pressure Vessel Technology* 193, no. 3 (2017): 134502.
[6] Kosinski, P., Kosinska, A. and Hoffman, A. "Fluid-particle flows in a driven cavity." In: *International Conference of*

Numerical Analysis and Applied Mathematics, 2006.
[7] Tey, W.Y. and Sidik, N.A.C. "A Review: The development of flapping hydrodynamics of body ad caudal fin movement fishlike structure." *Journal of Advanced Review on Scientific Research* 8, no. 1 (2015): 19-38.
[8] Patankar, S. "Numerical heat transfer and fluid flow." Washington: Hemisphere Pub. Corp, 1980.
[9] Yapici, K. and Uludag, Y. "Finite volume simulation of 2-d steady square lid driven cavity flow at high Reynolds numbers." *Brazilian Journal of Chemical Engineering*, 30, no. 4 (2013): 923-937.
[10] Yang, J., Guo, L. and Zhang, X. "A numerical simulation of pool boiling using CAS model." *International Journal of Heat and Mass Transfer* 46, no. 25 (2003): 4789-4797.
[11] Chow, W. and Cheung, Y. "Comparison of the algorithms PISO and SIMPLER for solving pressure-velocity linked equations in simulating compartmental fire." *Numerical Heat Transfer, Part A: Applications* 31, no. 1 (1997): 87-112.
[12] Versteeg, H. and Malalasekera, W. "An introduction to computational fluid dynamics." Harlow, England: Pearson Education Ltd, 2007.
[13] Ghia, U., Ghia, K. and Shin, C. "High-Re solutions for incompressible flow using the Navier-Stokes equations and a multigrid method."*Journal of Computational Physics*, 48, no. 3(1982): 387-411.
[14] Poochinapan, K. "Numerical implementations for 2d lid-driven cavity flow in stream function formulation." *ISRN Applied Mathematics*(2012): 1-17.